Title

Synthesis, characterization and reactivity of a Mn(III)-hydroxido complex as a biomimetic model for lipoxygenase.

Authors

Phu, Phan

Barman, Suman

Ziller, Joseph

et al.

Publication Date

2024-10-01

DOI

10.1016/j.jinorgbio.2024.112618

Peer reviewed

HHS Public Access

Author manuscript

J Inorg Biochem. Author manuscript; available in PMC 2024 October 24.

Published in final edited form as:

J Inorg Biochem. 2024 October ; 259: 112618. doi:10.1016/j.jinorgbio.2024.112618.

Synthesis, Characterization and Reactivity of a Mn(III)–hydroxido Complex as a Biomimetic Model for Lipoxygenase

Phan N. Phu[a], **Suman K. Barman**[a,b], **Joseph W. Ziller**[a], **Michael P. Hendrich**[c], **A. S. Borovik**[a,*]

[a]Department of Chemistry, University of California, Irvine, California 92697, United States

[b]Department of Chemical Sciences, India Institute of Science Education and Research (IISER) Mohali, Manauli 140306, India

[c]Department of Chemistry, Carnegie Mellon University, Pittsburgh, Pennsylvania 15213, United States

Abstract

Manganese hydroxido (Mn–OH) complexes supported by a tripodal *N,N',N''*-[nitrilotris(ethane-2,1-diyl)]tris(*P,P*-diphenylphosphinic amido) ([poat]$^{3-}$) ligand have been synthesized and characterized by spectroscopic techniques including UV-vis and electron paramagnetic resonance (EPR) spectroscopies. X-ray diffraction (XRD) methods were used to confirm the solid-state molecular structures of $\{Na_2[Mn^{II}poat(OH)]\}_2$ and $\{Na[Mn^{III}poat(OH)]\}_2$ as clusters that are linked by the electrostatic interactions between the sodium counterions and the oxygen atom of the ligated hydroxido unit and the phosphinic (P=O) amide groups of [poat]$^{3-}$. Both clusters feature two independent monoanionic fragments in which each contains a trigonal bipyramidal Mn center that is comprised of three equatorial deprotonated amide nitrogen atoms, an apical tertiary amine, and an axial hydroxido ligand. XRD analyses of $\{Na[Mn^{III}poat(OH)]\}_2$ also showed an intramolecular hydrogen bonding interaction between the Mn^{III}–OH unit and P=O group of [poat]$^{3-}$. Crystalline $\{Na[Mn^{III}poat(OH)]\}_2$ remains as clusters with Na^+---O interactions in solution and is unreactive towards external substrates. However, conductivity studies indicated that $[Mn^{III}poat(OH)]^-$ generated *in situ* is monomeric and reactivity studies found that it is capable of cleaving C–H bonds, illustrating the importance of solution-phase speciation and its direct effect on chemical reactivity.

Graphical Abstract

*Corresponding Author. aborovik@uci.edu.

CRediT authorship contribution statement

Phan N. Phu: Writing – original draft, review & editing, Methodology, Formal analysis, Data curation, Investigation, Visualization. **Suman K. Barman:** Methodology, Formal analysis, Data curation, Investigation. **Joseph W. Ziller:** Formal analysis, Data curation, Investigation. **Michael P. Hendrich:** Formal analysis, Data curation, Investigation, Funding acquisition. **A. S. Borovik:** Writing – review & editing, Conceptualization, Formal analysis, Investigation, Project administration, Supervision, Funding acquisition.

Declarations of competing interest

The authors declare no conflict of interest.

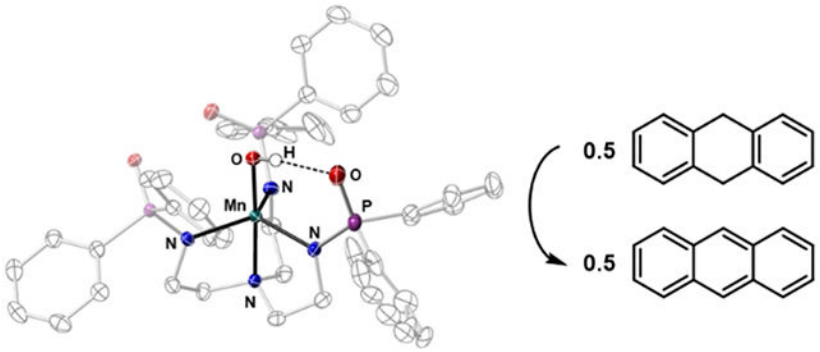

Synopsis:

Manganese–hydroxide complexes were synthesized to study the influence of H-bonds in the secondary coordination sphere and their effects on the oxidative cleavage of substrates containing C–H bonds.

Keywords

Mn–hydroxide; C–H bond cleavage; H-bonds; bioinspired coordination complexes; lipoxygenase; spectroscopy

1. Introduction

Manganese-dependent enzymes catalyze oxidative reactions critical for life and human health-related processes [1–3]. For instance, manganese superoxide dismutase functions as a vital antioxidant enzyme, protecting cellular organisms from oxidative stress by converting harmful superoxide radicals into O_2 and hydrogen peroxide [4]. In addition, manganese oxygenases utilize O_2 to facilitate enzymatic reactions by incorporating one or two oxygen atoms into external substrates. One example is lipoxygenase enzyme that catalyzes the hydroperoxidation of polyunsaturated fatty acids, a crucial step in the biosynthesis of plant signaling molecules [5–7]. One type of lipoxygenase contains a monomeric Mn center in which a terminal Mn^{III}–OH species is invoked as the kinetically competent intermediate in activating C–H bonds [7,8]. Studies on Mn lipoxygenases and related synthetic complexes have been aimed at determining the structure-function relationships that lead to efficient C–H bond functionalization. One outcome of these investigations is the prominent role of the secondary coordination sphere whereby non-covalent interactions, such as hydrogen bonds (H-bonds), assist in regulating reactivity [6,9,10]. Efforts to incorporate these features into synthetic Mn–OH complexes containing a terminal hydroxido ligand have proven to be challenging because H-bonds are relatively weak interactions, and thus difficult to install in a predictable and intramolecular manner. Moreover, there is a limited number of examples of structurally characterized Mn^{III}–OH complexes that show reactivity toward substrates with O–H bonds [11–15], with only $[Mn^{III}(OH)(PY5)]^{2+}$ (PY5 = 2,6-bis(bis(2-pyridyl)methoxymethane)pyridine) reported by Stack showing reactivity toward external substrates containing C–H bonds similar to those found for Mn lipoxygenase [16]. However, this complex does not have the ability to regulate the secondary coordination sphere; and

thus, the roles of secondary coordination sphere effects were not explored. Recent work from Jackson highlighted the importance of intramolecular H-bond within Mn^{III}–OH species in which the placement of a H-bond acceptor proximal to the hydroxide ligand substantially improved its reactivity toward substrates containing O–H bonds [17].

Our group has been developing tripodal ligands that promote intramolecular H-bond networks around metal centers. We have previously shown that the symmetrical urea-containing ligand $[H_3buea]^{3-}$ (Fig. 1A) can stabilize a Mn^{III}–OH complex with two intramolecular H-bonds formed between the urea NH groups (H-bond donors) and the O-atom of the hydroxide ligand (H-bond acceptor) [18,19]. We have also found that ligands containing phosphinic amido groups can serve as H-bond acceptors to Mn–OH groups and be used in the design of the hybrid tripodal ligand $[H_2pout]^{3-}$ [20]. Notice that the Mn^{III}–OH complex ($[Mn^{III}H_2pout(OH)]^{-}$, Fig. 1B) now has three intramolecular H-bonds involving the hydroxido ligand, which provided additional stability to the complex. Recently, we introduced the symmetrical phosphinic amido tripod, $[poat]^{3-}$, and found that it can be used to form a variety of mono- and dinuclear high valent Fe and Mn complexes [21–25]. In this report, we detail the preparation and characterization of mononuclear Mn–OH complexes and describe our continued efforts to understand the influence of secondary coordination spheres on the properties and reactivity of metal complexes. Our results demonstrate that $[poat]^{3-}$ can indeed stabilize Mn–OH complexes, and the intramolecular H-bond interaction between one P=O group of $[poat]^{3-}$ and the terminal Mn^{III}–OH unit (Fig. 1C) may play a role in its ability to cleave C–H bonds.

2. Experimental

General Procedures.

All experiments were carried out at room temperature unless otherwise noted. Syntheses of the metal complexes were carried out under an N_2 atmosphere in a Vacuum Atmospheres Co. dry box. Solvents were sparged with argon and purified using a JC Meyer Co. solvent purification system with columns containing Q-5 and molecular sieves. Dimethylformamide (DMF, Sigma-Aldrich) and dimethyl sulfoxide (DMSO, Honeywell Burdick & Jackson) were purchased and used without further purification. Sodium hydride (NaH) was purchased from Sigma-Aldrich as a 57–63% suspension in mineral oil and was washed on a 15-mL fine porosity glass frit with pentane (5 × 15 mL) and diethyl ether (Et_2O) (5 × 15 mL), dried under vacuum, and stored under an N_2 atmosphere. 9,10-dihydroanthracene (DHA) was purchased from Sigma-Aldrich, crystallized from ethanol, washed with pentane, and dried under vacuum. All other reagents were purchased from commercial suppliers and used as received. H_3poat was prepared according to a previously published procedure [21].

Physical Methods.

Electronic absorption spectra were collected in a 1 cm quartz cuvette and were performed on an Agilent Technologies Cary 60 Scan UV-vis spectrometer or an 8453 Agilent UV-vis spectrometer equipped with an Unisoku Unispeks cryostat. Solid-state Fourier transform infrared (FTIR) spectra were collected on a Thermo Scientific Nicolet iS5 spectrophotometer with an iD5 ATR attachment. Elemental analyses were performed on

a ThermoFisher FlashSmart CHNS/O Elemental Analyzer. X-band (microwave frequencies 9.28, 9.43, and 9.62 GHz) EPR spectra were collected on a Bruker EMX spectrometer equipped with an ER041XG microwave bridge, an Oxford Instrument liquid He 249 quartz cryostat, and a dual-mode (ER4116DM) or perpendicular-mode (ER4119HS-W1) cavity. Conductivity measurements were performed using Pt glass low-conductivity probe (Sper Scientific Direct). Organic products were detected by gas chromatography mass spectrometry (GC-MS) in the Mass Spectrometry Facility at the University of California, Irvine. Cyclic voltammetry experiments were conducted using a CHI600C electrochemical analyzer with 0.1 M tetrabutylammonium hexafluorophosphate ($[Bu_4N]PF_6$) as the supporting electrolyte. A 2.0 mm glassy carbon electrode and a platinum wire were used as the working and counter electrodes, respectively. A ferrocenium/ferrocene ($[FeCp_2]^{+/0}$) standard was used as an internal reference to monitor the reference ($Ag^{+/0}$) electrode.

Reactivity Studies:

In a glovebox under a N_2 atmosphere, 100 μL of a 20 mM DMSO solution of $[Mn^{II}poat(OH)]^{2-}$ was added to 1.9 mL of DMSO in a 1.0 cm pathlength quartz cuvette. The cuvette was sealed with a rubber septum, removed from the glovebox, and placed in an Agilent spectrometer equipped with a thermostat cell holder where it was equilibrated at 20 °C for 5 min. This solution was treated with 50 μL of a 40 mM solution of $[Fe^{III}Cp_2]BF_4$ via a gas-tight syringe. A kinetic experiment was initiated by injecting between 50 μL to 150 μL of a 470 mM solution of a substrate into the cuvette, also via a gas-tight syringe. The initial concentration of $Na_2[Mn^{II}poat(OH)]$ was set at 1.0 mM for all samples. The formation of the initial $[Mn^{III}poat(OH)]^-$ species in solution was monitored by following the increase in the absorption band at λ_{max} = 710 nm. The progress of the reaction with substrates was monitored by following the decrease in the absorbance at λ_{max} = 710 nm.

GC-MS Experiments for Organic Products:

Under a N_2 atmosphere, stirred solutions of $Na_2[Mn^{II}poat(OH)]$ were initially treated with 1 equivalent (equiv) of oxidant for 1 minute and 0.5 equiv of DHA was then added to the mixture. Within 5 minutes, the solutions changed from green to orange, after which the organic compounds were isolated by extraction with pentane (4 × 5 mL) for the DHA reaction and Et_2O (4 × 5 mL) for the xanthene reaction. The pentane or Et_2O layers were combined and passed through a short silica gel column, and the solvent was removed under reduced pressure to afford a white solid. The products were analyzed as dichloromethane (CH_2Cl_2) solution by GC-MS measurements in which hexamethylbenzene was used as the internal standard.

Synthesis of $Na_2[Mn^{II}poat(OH)]$.

A solution of H_3poat (415 mg, 0.555 mmol) in 6 mL of tetrahydrofuran (THF) was treated with NaH (39.9 mg, 1.66 mmol) and the cloudy white solution was stirred for 1 hour. To the reaction mixture, $Mn^{II}(OAc)_2$ (96.5 mg, 0.558 mmol) was added slowly. The mixture was stirred for 2 hours and was filtered through a fine-porosity glass-fritted funnel to afford a yellow filtrate and white solid on the glass frit (NaOAc, 91.1 mg, 1.11 mmol). H_2O (10 μL, 0.56 mmol) was added to the filtrate and the solution was stirred for 10 min. The reaction mixture was filtered through a fine porosity glass-fritted funnel, followed by the addition of

NaH (13.6 mg, 0.567 mmol) to yield a clear yellow solution after gas evolution ceased. THF was removed under vacuum to give a yellow oil, which was triturated with pentane to yield a white solid. The white solid was isolated by decanting the excess solvent and dried under vacuum (431 mg, 0.500 mmol, 90.4% yield). Light yellow crystals suitable for XRD study were obtained from a concentrated THF solution layered with pentane.

Elemental analysis for $Na_2[Mn^{II}poat(OH)]$, $C_{42}H_{43}MnN_4Na_2O_4P_3$, calculated: C, 58.54; H, 5.03; N 6.50%, found: C, 58.87; H, 5.24; N, 6.21%. EPR (X-band ⊥-mode, DMF:THF, 77 K): g = 5.7, 3.9, 2.0. FTIR (solid-state, cm^{-1}): 3625, 3442, 3253, 3166, 3110, 3033, 2446, 2166, 2100, 2020, 1975, 1871, 1786, 1681, 1634, 1432, 1362, 1311, 1222, 1160, 991, 950, 916, 891, 836.

$E_{1/2}$ (DMSO): i) 100 mV s^{-1}: –1.07 V (i_{pa}/i_{pc} = 1.13, ΔE = 135 mV) versus $[Fe^{III/II}Cp_2]^{+/0}$ (i_{pa}/i_{pc} = 1.01, ΔE = 95 mV); ii) at 50 mV s^{-1}: –1.07 V (i_{pa}/i_{pc} = 1.06, ΔE = 105 mV) versus $[Fe^{III/II}Cp_2]^{+/0}$ (i_{pa}/i_{pc} = 0.97, ΔE = 85 mV).

Synthesis of Na[Mn^{III}poat(OH)].

Route 1: $Na_2[Mn^{II}poat(OH)]$ (75.1 mg, 0.0872 mmol) was dissolved in ~4 mL of CH_2Cl_2 and treated with solid $[FeCp_2]BF_4$ (27.0 mg, 0.099 mmol). The reaction immediately turned dark green and was stirred for 10 minutes. The reaction was filtered through a pad of celite to remove a white solid byproduct and volatiles were removed under reduced pressure. The resultant dark green solid was rinsed with pentane 3–5 times to remove $Fe^{II}Cp_2$ and dried under vacuo. The resulting solid was redissolved in acetonitrile (CH_3CN), filtered, dried, and triturated with Et_2O to yield a green solid (66.2 mg, 0.0805 mmol, 89.5% yield).

Route 2: H_3poat (200. mg, 0.268 mmol) was dissolved in 3 mL of THF, and solid NaH (19.6 mg, 0.817 mmol) was added in one portion. The mixture was stirred for 1 hour and was treated with $Mn^{II}(OAc)_2$ (46.6 mg, 0.269 mmol). The solution was stirred for 2 hours to produce a yellow mixture which was filtered to remove white solid (NaOAc, 47.5 mg, 0.579 mmol) through a fine porosity glass-fritted funnel. The yellow filtrate was transferred to a Schlenk flask and sealed with a rubber septum. The mixture was treated with dry O_2 (3.2 mL, 0.133 mmol) via a gas-tight syringe to immediately produce a dark green solution and the solvent was removed under reduced pressure after 1 hour of stirring. The flask was returned to the glovebox where the solid was redissolved in minimal CH_3CN and stored at –35 °C to obtain green crystals suitable for XRD (21.6 mg, 0.0258 mmol, 10.0% yield). Elemental analysis for $Na[Mn^{III}poat(OH)]$, $C_{42}H_{43}MnN_4NaO_4P_3$, calculated: C, 60.15; H, 5.17; N 6.68%, found: C, 59.82; H, 5.25; N, 6.50%. EPR (X-band ||-mode, DMF:THF, 17 K): g = 8.0, A_z = 264 MHz. FTIR (solid-state, cm^{-1}): 3310, 3050, 2960, 2853, 2360, 2330, 1957, 1891, 1815, 1587, 1436, 1183, 1112, 958, 783, 745, 716, 700. UV-vis (DMSO, λ_{max} nm, (ε_M) = 444 (294), 710 (880).

3. Results and Discussion

3.1. Preparation and properties of Na$_2$[Mn^{II}poat(OH)].

The $Na_2[Mn^{II}poat(OH)]$ salt was synthesized according to a method we reported previously (Scheme 1) [23]. The salt was prepared by treating an anhydrous THF solution of H_3poat

with three equiv of NaH for 30–45 min before the addition of 1 equiv of $Mn^{II}(OAc)_2$. After the removal of the NaOAc byproduct via filtration, the yellow filtrate was treated with 1 equiv of degassed H_2O, followed by the addition of 1 equiv of NaH to generate $Na_2[Mn^{II}poat(OH)]$. The volatiles were removed under reduced pressure and the resultant mixture was triturated with pentane to afford $Na_2[Mn^{II}poat(OH)]$ as a yellow solid in 90% yield. A THF solution of this salt was layered under pentane to afford single crystals suitable for XRD methods.

The perpendicular-mode EPR spectrum of $[Mn^{II}poat(OH)]^{2-}$ displayed a signal consistent with the assignment of a high-spin ($S = 5/2$) Mn center (Fig. 2A) [20,26,27]. The complex did not exhibit any transitions in the UV-visible region, supporting a d^5 ground-state electronic configuration of Mn^{II}. The solid-state vibrational properties of the $[Mn^{II}poat(OH)]^{2-}$ complex were studied using FTIR spectroscopy. The complex showed a ν(O–H) vibration at 3625 cm^{-1} (Fig. S1), which is comparable to that of Mn^{II}–OH complexes in related systems [20].

3.2. Preparation and properties of Na[Mn^{III}poat(OH)].

The preparative route of $Na[Mn^{III}poat(OH)]$ was also crafted from a previous synthesis that utilized chemical oxidants such as I_2 and $[FeCp_2]^+$ (Scheme 1) [20]. Green crystals of this salt were obtained from a concentrated CH_3CN solution of the compound at –35 °C. The parallel-mode EPR spectrum of $Na[Mn^{III}poat(OH)]$ displayed a feature centered at $g = 8.0$ with a six-line pattern (^{55}Mn hyperfine constant (A_{iso}) = 264 MHz) (Fig. 2B) that is characteristic of a mononuclear Mn^{III} complex with an $S = 2$ spin ground state [20,26]. The UV-vis spectrum of $Na[Mn^{III}poat(OH)]$ showed two peaks at λ_{max} (ε_M) = 444 (294) and 710 (880) nm (Fig. 2C) and are comparable to optical properties of other Mn^{III}–OH complexes in trigonal bipyramidal (tbp) geometry [18–20,28]. The FTIR spectrum of this complex revealed a peak at 3442 cm^{-1} that is attributed to the O–H vibration (Fig. S1).

3.3. Solid-state molecular structures of {$Na_2[Mn^{II}poat(OH)]$}$_2$ and {$Na[Mn^{III}poat(OH)]$}$_2$.

The molecular structures of both salts were determined by XRD methods. In the crystalline phase, the anionic fragments of the Mn–OH species are part of clusters with that are formulated as $\{Na_2[Mn^{II}poat(OH)]\}_2$ and $\{Na[Mn^{III}poat(OH)]\}_2$ (Fig. 3A and C; and Tables 1 and S1). The Mn centers in both clusters are coordinated by the $[poat]^{3-}$ ligand in a tetradentate fashion with three deprotonated phosphinic amido N-atoms (N2, N3, N4) and an apical N-atom (N1). A truncated view of $Na_2[Mn^{II}poat(OH)]$ (Fig. 3B) shows that the remaining coordination site on the Mn center is occupied by a hydroxido ligand to render a Mn^{II}–OH anion with a nearly ideal tbp geometry, as gauged by a trigonal structural parameter (τ_5) value of 1.008 (where $\tau_5 = 1$ for tbp and 0 for square pyramidal geometry). The Mn1–O1 and Mn1–N1 distances of 2.091(1) and 2.453(2) Å are comparable to those reported for similar Mn^{II}–OH complexes [18,20,29]; for instance, Mn1–O1 and Mn1–N1 distances of 2.051(1) and 2.315(1) Å were found in $[Mn^{II}H_2pout(OH)]^{2-}$ (Table S2) [20]. The molecular structure of $\{Na_2[Mn^{II}poat(OH)]\}_2$ (Fig. 3A) also revealed electrostatic interactions between the Na^+ ions and the O atoms of $[poat]^{3-}$ and hydroxido ligand that appears to promote aggregation. This type of interaction is similar to what we observed in the molecular structures of the corresponding Fe^{II}, Fe^{III}, and Fe^{III}–OH complexes of

[poat]$^{3-}$ that also crystallized as aggregates [22,23], emphasizing the ability of the P=O unit within a phosphinic amido group to bind metal ions. The molecular structure further showed that Na^+---O=P interactions appeared to prevent the formation of intramolecular H-bonds between the [poat]$^{3-}$ ligand and the Mn^{II}–OH unit.

The $\{Na[Mn^{III}poat(OH)]\}_2$ cluster also contains two monoanionic fragments that are linked through two Na^+ ions coordinated to the O atoms of the hydroxido and P=O units of the $[Mn^{III}poat(OH)]^-$ complexes (Fig. 3C and D; and Table S1). Similar to $\{Na_2[Mn^{II}poat(OH)]\}_2$, each monoanionic fragment in $\{Na[Mn^{III}poat(OH)]\}_2$ contains a Mn center with tbp coordination geometry with a τ_5 value of 0.915. The Mn1–O1 bond distance of 1.829(2) Å is comparable to those found in other Mn^{III}–OH complexes[14,16,18,20,30] and is significantly shorter than that found in $\{Na_2[Mn^{II}poat(OH)]\}$ (Tables 1 and S2), in agreement with a change in the oxidation state. Moreover, the Mn1–N1 and Mn1–N_{eq} bond distances in the Mn^{III}–OH complex also exhibit the expected contraction compared to those in the Mn^{II}–OH analog (Table 1). Furthermore, the distance between the O1 and O2 of the P=O in [poat]$^{3-}$ is 2.803(3) Å, placing them within the range of a H-bond.

3.4. Redox properties and preliminary reactivity studies of Mn^{III}–OH complex with C–H bonds.

The redox properties of the Mn^{II}–OH complex were investigated by cyclic voltammetry in DMSO solution containing $[Bu_4N]PF_6$ as the electrolyte. The cyclic voltammogram of $[Mn^{II}poat(OH)]^{2-}$ (Fig. 4A) showed a reversible one-electron event at an $E_{1/2}$ = –1.07 V versus $[FeCp_2]^{+/0}$ that is assigned to the $Mn^{III/II}$–OH redox couple. As discussed above, Mn^{III}–OH species are known to perform allylic C–H bond oxidation in lipoxygenase [6,7]. Therefore, we sought to test the activity of $[Mn^{III}poat(OH)]^-$ towards organic substrates containing weak C–H bonds such as DHA (C–H bond dissociation energy (BDE) = 78 kcal mol^{-1} and pK_a = 30). Treating a solution of $[Mn^{III}poat(OH)]^-$ (prepared by treating $[Mn^{II}poat(OH)]^{2-}$ with $[Fe^{III}Cp_2]^+$ in DMSO) resulted in rapid decay of its characteristic band at λ_{max} = 710 nm concomitantly with the new growth of new absorption peaks at λ_{max} = 343, 360, and 380 nm that indicated formation of anthracene (Fig. 4B). Analysis of the reaction mixture by GC-MS found anthracene (70% conversion) as the only product (Fig. S2A). Under the same experimental conditions, $[Mn^{III}poat(OH)]^-$ was found to oxidize xanthene (C–H BDE = 75 kcal mol^{-1} and pK_a = 30) to generate 9,9'-bixanthene (86% conversion, Fig. S2B). However, treatment of $[Mn^{III}poat(OH)]^-$ with fluorene (BDE = 80 kcal mol^{-1} and pK_a = 23) did not lead to C–H bond cleavage; rather, deprotonation of fluorene was observed as determined by the appearance of optical features at λ_{max} = 454, 485, and 520 nm that are consistent with the formation of the fluorene anion (Fig. S3). On the other hand, no reactivity was observed when DMSO solutions of re-dissolved $\{Na[Mn^{III}poat(OH)]\}_2$ crystals were treated with DHA, even in the presence of 15-crown-5 or 2,2,2-cryptand. It is possible that using crystalline samples would produce solutions of intact $\{Na[Mn^{III}poat(OH)]\}_2$ clusters that could be inactive toward cleaving C–H bonds from external substrates. To evaluate this premise, we used conductivity studies to probe the speciation of crystalline and *in situ* generated Mn^{III}–OH complex in solution and analyzed our data using the Onsager relationship (see SI and eqs S1–S2) [31]. The persistence

of the $\{Na[Mn^{III}poat(OH)]\}_2$ cluster in solutions of redissolved crystals is supported by conductivity data that is nearly constant as a function of increasing concentration (Fig. S4 and Table S3), a behavior that is consistent with known non-electrolyte. In contrast, an increase in conductivity was observed for the solution in which the $[Mn^{III}poat(OH)]^-$ complex was generated *in situ*, and an Onsager plot produced a line with a slope similar to that of a related 1:1 electrolyte (Fig. S5 and Table S4), suggesting the presence of a monomeric anion in solution (that is, a discrete $[Mn^{III}poat(OH)]^-$ species).

Cleavage of C–H bonds by synthetic Mn^{III}–OH models is rare, with only one example of a $[Mn^{III}(PY5)(OH)]^{2+}$ complex reported by Stack capable of oxidizing DHA [16]. The $[Mn^{III}poat(OH)]^-$ complex in this study represents a biomimetic model of lipoxygenase that is not only capable of C–H bond oxidation, but also incorporates intramolecular H-bonding interactions that have shown to be important for enzymatic functions. The presence of H-bond acceptors in the secondary coordination sphere of $[Mn^{III}poat(OH)]^-$ may be important for its reactivity when compared to a tbp Mn^{III}–OH complex, $[Mn^{III}H_3buea(OH)]^-$, that contains three H-bond donors in the secondary coordination sphere and is inactive toward DHA [19]. In contrast, the mononuclear Mn^{III}–oxo complex supported by the same scaffold, $[Mn^{III}H_3buea(O)]^{2-}$ [19,32,33], can perform C–H bond oxidation of the same substrate. The difference in reactivity between $[Mn^{III}H_3buea(OH)]^-$ and $[Mn^{III}poat(OH)]^-$ may also be a function of the differing basicity of the Mn^{III}–OH units, which is known to be influenced by the intramolecular H-bonding network [17,27,34–36]. Therefore, exploration of the mechanistic pathway in hydrocarbon oxidation and understanding the role of H-bonding in $[Mn^{III}poat(OH)]^-$ reactivity is necessary.

4. Conclusions

We have described the synthesis and characterization of $Na_2[Mn^{II}poat(OH)]$ and $Na[Mn^{III}poat(OH)]$ complexes containing terminal Mn–OH units. The electrostatic interactions of the Na^+ counterion with the oxygen atom of the Mn–hydroxido unit and the P=O groups promoted the formation of $\{Na_2[Mn^{II}poat(OH)]\}_2$ and $\{Na[Mn^{III}poat(OH)]\}_2$ aggregates in the solid state. The $[poat]^{3-}$ ligand supported the formation of high-spin Mn species, as determined by EPR spectroscopy. Reactivity studies showed that $[Mn^{III}poat(OH)]^-$, generated *in situ* from the oxidation of $[Mn^{II}poat(OH)]^{2-}$, can cleave C–H bonds in DHA and xanthene; however, when the complex was part of a cluster, no reactivity was observed.

$[Mn^{III}poat(OH)]^-$ represents a biomimetic model of Mn lipoxygenase that is not only capable of cleaving C–H bonds but also incorporates H-bonds to the Mn–OH unit that are reminiscent of non-covalent interactions found within the active sites of metalloproteins. Our findings offer insights into the structural factors of H-bonds that possibly help regulate function. In particular, the presence of H-bond acceptors within the secondary coordination sphere may assist in promoting the cleavage of C–H bonds. We have previously shown that $[Mn^{III}H_3buea(OH)]^-$ does not react with external substrates containing C–H bonds: in this complex, the hydroxido ligand serves as a H-bond acceptor for the urea NH groups, which appears to provide sufficient stabilization to cause the complex to be inactive. For $[Mn^{III}poat(OH)]^-$, the hydroxido ligand is the H-bond donor to the $[poat]^{3-}$ ligand which

would alter its properties, such as making the Mn–OH unit more basic. We have already demonstrated the importance of the basicity of Mn–O and Mn–OH complexes in cleaving C–H bonds and point to our studies on the Mn^{III}–oxido complex, $[Mn^{III}H_3buea(O)]^-$, which readily reacts with external substrates such as DHA and xanthene. The basicity of the Mn–oxido unit in this type of complex is controllable with intramolecular H-bonds that we have shown was correlated with rate [27]. Having the hydroxido ligand as the H-bond acceptor in $[Mn^{III}poat(OH)]^-$ would produce a more "oxido" like ligand and increase its reactivity by rendering a more basic complex.

Supplementary Material

Refer to Web version on PubMed Central for supplementary material.

Acknowledgements

We thank the National Institutes of Health USA (GM050781 to A.S.B. and GM141948 to M.P.H.) for financial support and the UCI Department of Chemistry for a fellowship to P.N.P. This paper is dedicated to Larry Que, Jr.

References

[1]. Yano J, Yachandra V, Mn_4Ca cluster in photosynthesis: Where and how water is oxidized to dioxygen, Chem. Rev 114 (2014) 4175–4205. 10.1021/cr4004874. [PubMed: 24684576]

[2]. Zhu W, Richards NGJ, Biological functions controlled by manganese redox changes in mononuclear Mn-dependent enzymes, Essays Biochem. 61 (2017) 259–270. 10.1042/EBC20160070. [PubMed: 28487402]

[3]. Schmidt SB, Husted S, The biochemical properties of manganese in plants, Plants 8 (2019) 381. 10.3390/plants8100381. [PubMed: 31569811]

[4]. Sheng Y, Abreu IA, Cabelli DE, Maroney MJ, Miller AF, Teixeira M, Valentine JS, Superoxide dismutases and superoxide reductases, Chem. Rev 114 (2014) 3854–3918. 10.1021/cr4005296. [PubMed: 24684599]

[5]. Hamberg M, Chao S, Oliw E, Manganese Lipoxygenase: Discovery of a bis-allylic hydroperoxide as product and intermediate in a lipoxygenase reaction, J. Biol. Chem 273 (1998) 13080–13088. 10.1074/jbc.273.21.13080. [PubMed: 9582346]

[6]. Wennman A, Oliw EH, Karkehabadi S, Chen Y, Crystal structure of manganese lipoxygenase of the rice blast fungus Magnaporthe oryzae, J. Biol. Chem 291 (2016) 8130–8139. 10.1074/jbc.M115.707380. [PubMed: 26783260]

[7]. Oliw EH, Iron and manganese lipoxygenases of plant pathogenic fungi and their role in biosynthesis of jasmonates, Arch. Biochem. Biophys 722 (2022) 109169. 10.1016/j.abb.2022.109169. [PubMed: 35276213]

[8]. Offenbacher AR, Holman TR, Fatty acid allosteric regulation of C-H activation in plant and animal lipoxygenases, Molecules 25 (2020) 3374. 10.3390/molecules25153374. [PubMed: 32722330]

[9]. Neidig ML, Wecksler AT, Schenk G, Holman TR, Solomon EI, Kinetic and spectroscopic studies of N694C lipoxygenase: A probe of the substrate activation mechanism of a nonheme ferric enzyme, J. Am. Chem. Soc 129 (2007) 7531–7537. 10.1021/ja068503d. [PubMed: 17523638]

[10]. Schurmann K, Anton M, Ivanov I, Richter C, Kuhn H, Walther M, Molecular basis for the reduced catalytic activity of the naturally occurring T560M mutant of human 12/15-lipoxygenase that has been implicated in coronary artery disease, J. Biol. Chem 286 (2011) 23920–23927. 10.1074/jbc.M110.211821. [PubMed: 21558275]

[11]. Coggins MK, Brines LM, Kovacs JA, Synthesis and structural characterization of a series of $Mn^{III}OR$ complexes, including a water-soluble $Mn^{III}OH$ that promotes aerobic hydrogen-atom transfer, Inorg. Chem 52 (2013) 12383–12393. 10.1021/ic401234t. [PubMed: 24156315]

[12]. Zhang J, Lee YM, Seo MS, Kim Y, Lee E, Fukuzumi S, Nam W, Oxidative versus basic asynchronous hydrogen atom transfer reactions of Mn(III)-hydroxo and Mn(III)-aqua complexes, Inorg. Chem. Front 9 (2022) 3233–3243. 10.1039/d2qi00741j.

[13]. Reed CJ, Agapie T, Thermodynamics of proton and electron transfer in tetranuclear clusters with Mn–OH_2/OH motifs relevant to H_2O activation by the Oxygen Evolving Complex in Photosystem II, J. Am. Chem. Soc 140 (2018) 10900–10908. 10.1021/jacs.8b06426. [PubMed: 30064207]

[14]. Wijeratne GB, Corzine B, Day VW, Jackson TA, Saturation kinetics in phenolic O–H bond oxidation by a mononuclear Mn(III)–OH complex derived from dioxygen, Inorg. Chem 53 (2014) 7622–7634. 10.1021/ic500943k [PubMed: 25010596]

[15]. Moore SM, Sun C, Steele JL, Laaker EM, Rheingold AL, Doerrer LH, HAA by the first {Mn(III)OH} complex with all O-donor ligands, Chem. Sci 14 (2023) 8187–8195. 10.1039/d3sc01971c. [PubMed: 37538819]

[16]. Goldsmith CR, Cole AP, Stack TDP, C–H activation by a mononuclear manganese(III) hydroxide complex: Synthesis and characterization of a manganese-lipoxygenase mimic?, J. Am. Chem. Soc 127 (2005) 9904–9912. 10.1021/ja039283w. [PubMed: 15998097]

[17]. Opalade AA, Hessefort L, Day VW, Jackson TA, Controlling the reactivity of a metal-hydroxo adduct with a hydrogen bond, J. Am. Chem. Soc 143 (2021) 15159–15175. 10.1021/jacs.1c06199. [PubMed: 34494835]

[18]. Shirin Z, Hammes BS, Young VG, Borovik AS, Hydrogen bonding in metal oxo complexes: Synthesis and structure of a monomeric manganese(III)–oxo complex and its hydroxo analogue, J. Am. Chem. Soc 122 (2000) 1836–1837.

[19]. Gupta R, MacBeth CE, Young VG, Borovik AS, Isolation of monomeric $Mn^{III/II}$–OH and Mn^{III}–O complexes from water: Evaluation of O–H bond dissociation energies, J. Am. Chem. Soc 124 (2002) 1136–1137. 10.1021/ja016741x. [PubMed: 11841259]

[20]. Oswald VF, Weitz AC, Biswas S, Ziller JW, Hendrich MP, Borovik AS, Manganese–hydroxido complexes supported by a urea/phosphinic amide tripodal ligand, Inorg. Chem 57 (2018) 13341–13350. 10.1021/acs.inorgchem.8b01886. [PubMed: 30299920]

[21]. Oswald VF, Lee JL, Biswas S, Weitz AC, Mittra K, Fan R, Li J, Zhao J, Hu MY, Alp EE, Bominaar EL, Guo Y, Green MT, Hendrich MP, Borovik AS, Effects of noncovalent interactions on high-spin Fe(IV)–oxido Complexes, J. Am. Chem. Soc 142 (2020) 11804–11817. 10.1021/jacs.0c03085. [PubMed: 32489096]

[22]. Sun C, Oswald VF, Hill EA, Ziller JW, Borovik AS, Investigation of iron–ammine and amido complexes within a C_3-symmetrical phosphinic amido tripodal ligand, Dalt. Trans 50 (2021) 11197–11205. 10.1039/d1dt01032h.

[23]. Lee JL, Oswald VF, Biswas S, Hill EA, Ziller JW, Hendrich MP, Borovik AS, Stepwise assembly of heterobimetallic complexes: synthesis, structure, and physical properties, Dalt. Trans 50 (2021) 8111–8119. 10.1039/d1dt01021b.

[24]. Lee JL, Biswas S, Sun C, Ziller JW, Hendrich MP, Borovik AS, Bioinspired di-Fe complexes: Correlating structure and proton transfer over four oxidation states, J. Am. Chem. Soc 144 (2022) 4559–4571. 10.1021/jacs.1c12888. [PubMed: 35192354]

[25]. Lee JL, Biswas S, Ziller JW, Bominaar EL, Hendrich MP, Borovik AS, Accessing a synthetic $Fe^{III}Mn^{IV}$ core to model biological heterobimetallic active sites, Chem. Sci 15 (2024) 2817–2826. 10.1039/d3sc04900k. [PubMed: 38404374]

[26]. Gupta R, Taguchi T, Borovik AS, Hendrich MP, Characterization of monomeric $Mn^{II/III/IV}$–hydroxo complexes from X- and Q-band dual mode electron paramagnetic resonance (EPR) spectroscopy, Inorg. Chem 52 (2013) 12568–12575. 10.1021/ic401681r. [PubMed: 24156406]

[27]. Barman SK, Jones JR, Sun C, Hill EA, Ziller JW, Borovik AS, Regulating the basicity of metal–oxido Complexes with a single hydrogen bond and its effect on C–H bond cleavage, J. Am. Chem. Soc 141 (2019) 11142–11150. 10.1021/jacs.9b03688. [PubMed: 31274298]

[28]. Rice DB, Wijeratne GB, Burr AD, Parham JD, Day VW, Jackson TA, Steric and electronic influence on proton-coupled electron-transfer reactivity of a mononuclear Mn(III)-hydroxo complex, Inorg. Chem 55 (2016) 8110–8120. 10.1021/acs.inorgchem.6b01217. [PubMed: 27490691]

[29]. Park YJ, Matson EM, Nilges MJ, Fout AR, Exploring Mn–O bonding in the context of an electronically flexible secondary coordination sphere: Synthesis of a Mn(III)–oxo, Chem. Commun 51 (2015) 5310–5313. 10.1039/c4cc08603a.

[30]. Eichhorn DM, Armstrong WH, A remarkably stable mononuclear manganese(III) hydroxide complex: [$L^1Mn^{III}(OH)$] [H_2L^1 = bis(2-hydroxy-5-nitrobenzyliminopropyl)methylamine], J. Chem. Soc., Chem. Commun (1992) 85–87.

[31]. Geary WJ, The use of conductivity measurements in organic solvents for the characterisation of coordination compounds, Coord. Chem. Rev 7 (1971) 81–122. 10.1016/S0010-8545(00)80009-0.

[32]. Gupta RR, Borovik AS, Monomeric $Mn^{III/II}$ and $Fe^{III/II}$ Complexes with terminal hydroxo and oxo ligands: Probing reactivity via O–H Bond dissociation energies, J. Am. Chem. Soc 125 (2003) 13234–13242. 10.1021/ja030149l. [PubMed: 14570499]

[33]. Parsell TH, Yang MY, Borovik AS, C–H bond cleavage with reductants: Re-investigating the reactivity of monomeric $Mn^{III/IV}$–oxo complexes and the role of oxo ligand basicity, J. Am. Chem. Soc 131 (2009) 2762–2763. 10.1021/ja8100825. [PubMed: 19196005]

[34]. Ehudin MA, Quist DA, Karlin KD, Enhanced rates of C–H Bond cleavage by a hydrogen-bonded synthetic heme high-valent iron(IV) oxo complex, J. Am. Chem. Soc 141 (2019) 12558–12569. 10.1021/jacs.9b01253. [PubMed: 31318198]

[35]. Ortmayer M, Hardy FJ, Quesne MG, Fisher K, Levy C, Heyes DJ, Catlow CRA, De Visser SP, Rigby SEJ, Hay S, Green AP, A noncanonical tryptophan analogue reveals an active site hydrogen bond controlling ferryl reactivity in a heme peroxidase, JACS Au 1 (2021) 913–918. 10.1021/jacsau.1c00145. [PubMed: 34337604]

[36]. Follmer AH, Borovik AS, The role of basicity in selective C–H bond activation by transition metal-oxidos, Dalt. Trans 52 (2023) 11005–11016. 10.1039/D3DT01781H.

Highlights

- A synthetic Mn^{III}–OH complex capable of C–H bond cleavage is reported
- Reactivity of Mn^{III}–OH complexes with H-bond acceptors
- Modulating the secondary coordination sphere of metal-hydroxide complexes

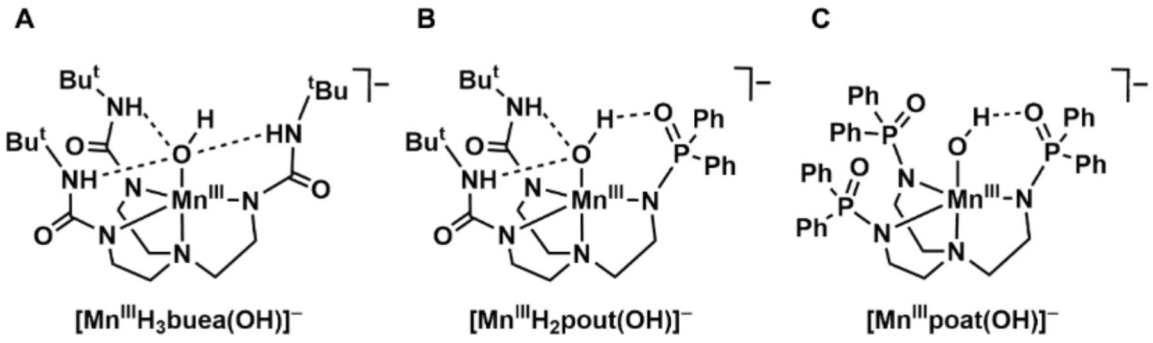

Fig. 1.
Mn^{III}–OH complexes supported by $[H_3buea]^{3-}$ (A), $[H_2pout]^{3-}$ (B), and $[poat]^{3-}$ (C).

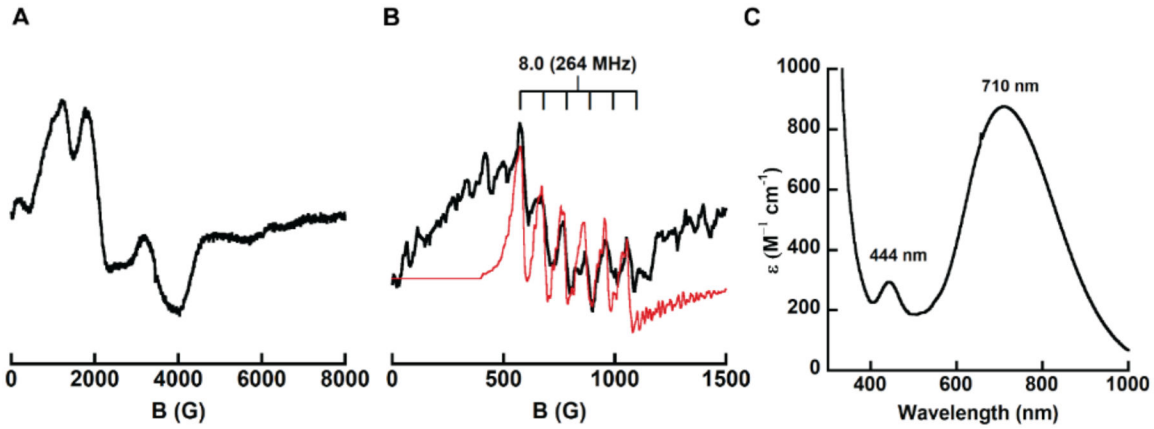

Fig. 2.

(A) ⊥-mode EPR spectrum of $Na_2[Mn^{II}poat(OH)]$ and (B) ||-mode EPR spectrum of $Na[Mn^{III}poat(OH)]$ with simulation in red collected at 17K in a 1:1 mixture of DMF:THF. (C) UV-vis spectrum of $Na[Mn^{III}poat(OH)]$ in DMSO at 20 °C.

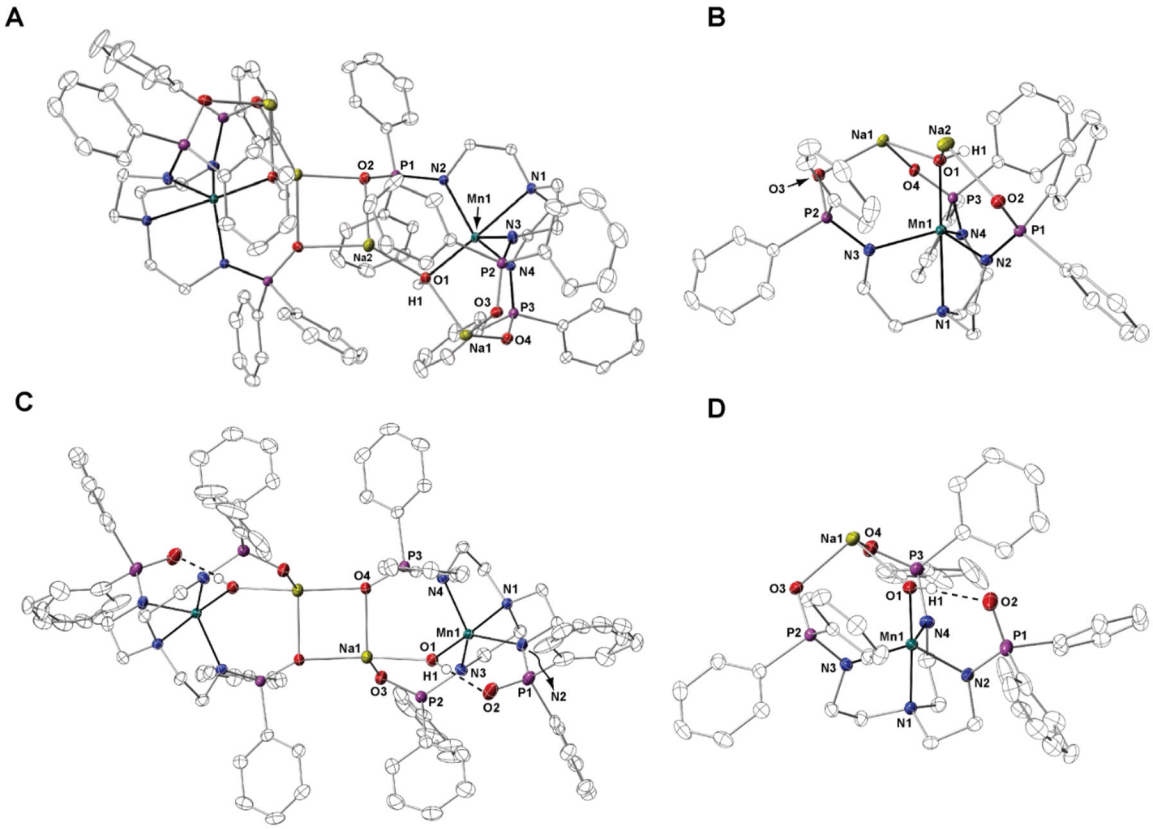

Fig. 3.

Thermal ellipsoid diagrams depicting the molecular structures of $\{Na_2[Mn^{II}poat(OH)]\}_2$ (A), $Na_2[Mn^{II}poat(OH)]$ (B), $\{Na[Mn^{III}poat(OH)]\}_2$ (C), and $Na[Mn^{III}poat(OH)]$ (D). The ellipsoids are drawn at 50% probability level, and only the hydroxido H atoms are shown for clarity.

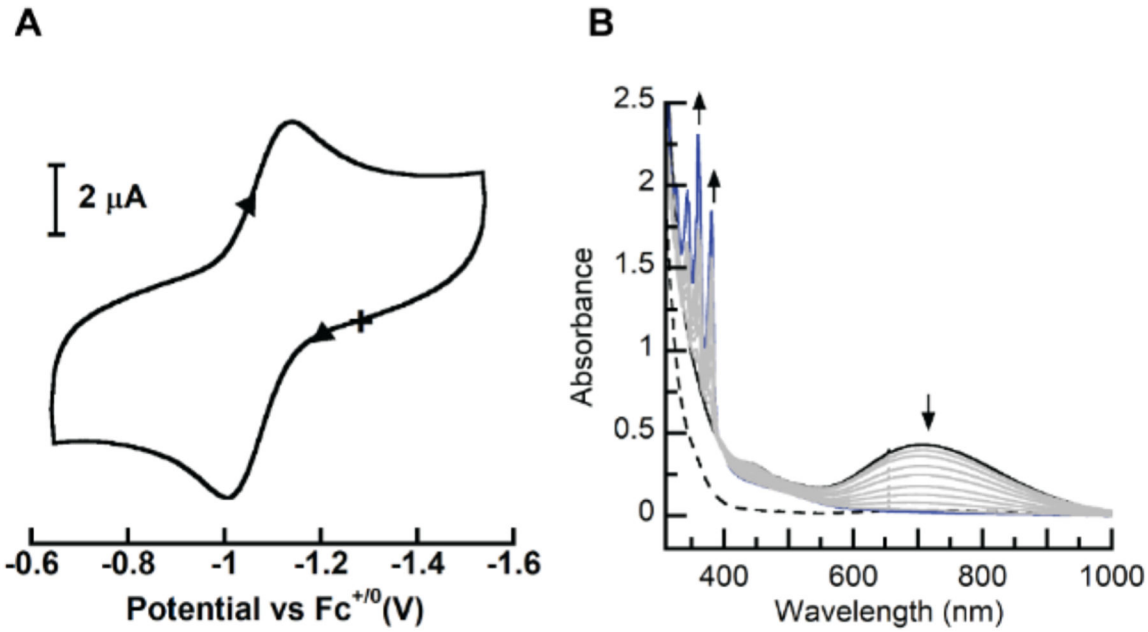

Fig. 4.

Cyclic voltammogram of $[Mn^{II}poat(OH)]^{2-}$ collected at a scan rate of 100 mV s^{-1} in DMSO (A). UV-vis spectrum of $[Mn^{II}poat(OH)]^{2-}$ (dashed) and upon oxidation with $[FeCp_2]^+$ to generate $[Mn^{III}poat(OH)]^-$ (black) and the spectral changes after addition of DHA to generate anthracene (blue) in DMSO at 20 °C (B).

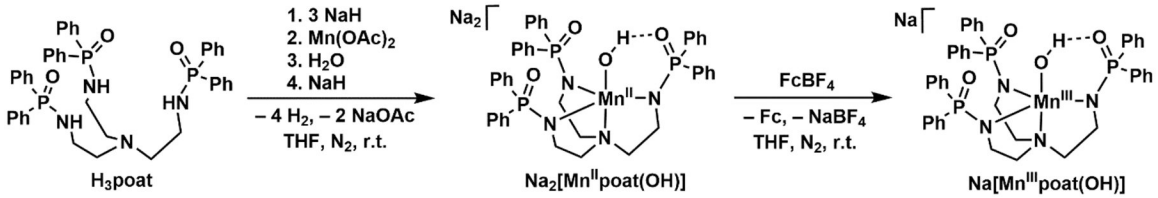

Scheme 1.
Preparation of $Na_2[Mn^{II}poat(OH)]$ and $Na[Mn^{III}poat(OH)]$.

Table 1

Selected bond lengths/distances (Å) and angles (°) for the $[Mn^{II/III}(OH)]^{2-/1-}$ complexes.[a]

	$Na_2[Mn^{II}poat(OH)]$	$Na[Mn^{III}poat(OH)]$
	Bond Lengths (Å)	
Mn1–N1	2.453(2)	2.050(2)
Mn1–N2	2.176(2)	2.072(2)
Mn1–N3	2.179(2)	2.047(2)
Mn1–N4	2.156(2)	2.063(2)
Mn1–O1	2.091(1)	1.829(2)
O1 ··· O2	---	2.803(3)
av $Mn1–N_{eq}$	2.170(2)	2.061(2)
	Angles (°)	
O1–Mn1–N1	178.07(5)	177.35(8)
N2–Mn1–N1	75.23(5)	80.97(8)
N3–Mn1–N1	77.34(5)	81.79(7)
N4–Mn1–N1	74.87(5)	82.07(8)
N4–Mn1–N2	117.58(6)	113.42(8)
N2–Mn1–N3	114.94(6)	117.87(8)
N4–Mn1–N3	109.96(6)	122.43(8)
	Calculated Values	
τ_5 [b]	1.008	0.915

[a] Bond lengths, distances, and angles are reported as an average.

[b] Trigonality structural parameter, $\tau_5 = (\beta - \alpha)/60°$.

β is the largest bond angle observed, and α is the second largest bond angle observed.